Journal of Membrane Science 415–416 (2012) 784–792

Contents lists available at SciVerse ScienceDirect

Journal of Membrane Science

journal homepage: www.elsevier.com/locate/memsci

Preparation of bi-continuous macroporous polyamide copolymer membranes for cell culture

Trong-Ming Don [a,b], Yi-Chun Hsu [a], Hung-Yin Tai [a], Earl Fu [c], Liao-Ping Cheng [a,b,*]

[a] Department of Chemical and Materials Engineering, Tamkang University, New Taipei city 25137, Taiwan
[b] Energy and Opto-Electronic Materials Research Center, Tamkang University, New Taipei city 25137, Taiwan
[c] Department of Periodontology, School of Dentistry, National Defense Medical Center and Tri-service General Hospital, Taiwan

ARTICLE INFO

Article history:
Received 26 April 2012
Received in revised form
29 May 2012
Accepted 29 May 2012
Available online 6 June 2012

Keywords:
Chitosan
Porous membrane
Nylon copolymer
Cell culture
Scaffold

ABSTRACT

Skinless bi-continuous macroporous membranes with extremely high porosity, ~80%, were prepared by the non-solvent induced phase separation (NIPS) process, from casting dopes composed of Elvamide (co-polymer of Nylon-6, -66, and -610), chitosan, and formic acid that were immersed in a water bath maintained at 10 °C. The Chitosan, while functioned as a pore former, migrated along with out-diffusing formic acid into the bath during the NIPS process, thereby, breaking the top gel-layer and the boundaries between cellular pores to yield a morphology featuring interpenetration networks of pores and polymer host. The amount of chitosan added to the dope affected significantly the pore size and porosity of the membranes formed, as revealed by SEM observations. At the highest chitosan/Elvamide ratio of 0.155, very large pore size (~30 μm) and porosity (83%) were achieved, whereas at the lowest ratio of 0.1, the membrane became asymmetric, and the pore size was reduced to ~15 μm. ^{1}H NMR analyses indicated that chitosan was completely removed during the precipitation process. Furthermore, L929 cells were cultured on various porous membranes. It is interesting to find that this cell was able to dwell on the pore walls in the cross sectional region, although with a smaller proliferation than on a flat nonporous surface.

1. Introduction

Polymeric membranes with appropriate 3-D porous structures are extensively used in tissue engineering as scaffolds for culturing of cells [1–2]. Unlike ordinary micro- or nano-porous membranes applied in various fine separation operations, the scaffold membranes have to be skinless and are characterized by high porosity, large pore size, and good pore–pore interconnectivity, in addition to biocompatibility and possibly biodegradability [3]. However, successful preparation of such special kind of porous structure is rather difficult, and is often considered as a matter of 'art'. In fact, how to produce porous membranes suited to tissue regenerating applications is a topic under enthusiastic exploration currently.

A number of methods have been developed for the preparation of porous membranes over the past few decades, such as phase separation [4–9], gas foaming [10–12], 3D printing [13], porogen leaching, etc. [14–25]. In a typical phase separation process, an initially homogeneous polymer solution (dope) is brought to a thermodynamically unstable state by means of contacting a non-solvent (Non-solvent Induced Phase Separation, NIPS) or by lowering temperature of the dope (Thermally Induced Phase Separation, TIPS). In either case, phase separation takes place in the form of liquid–liquid demixing and/or polymer crystallization, depending on the phase behavior and the preparative parameters, to yield polymer-poor and polymer-rich phases. Subsequent development of these separated phases leads to various porous morphologies in the membrane [3,26].

For the NIPS process, addition of pore formers in the dope is a common practice to change the pore size, pore structure, and porosity of the membranes. Some kind of pore formers actually involve in the phase separation process, e.g., addition of non-solvent in the dope to induce crystallization [22,23], while others may be quite passive, being used just to occupy temporarily a space, which later on become pores after removal of the additives [21,24,25]. A wide variety of materials have been shown to be effective pore formers, such as poly(vinyl pyrrolidone) [15], polyethylene glycol [14,15], hyper-branched polymers [14], inorganic salts [16–20], silica particles [21], organically modified clays [25], different aggregated state of water [22,23], etc. Although the pore size and porosity can be controlled by proper application of these pore formers [27], symmetric membranes with pores that interconnect into networks of continuous channels are still difficult to prepare, particularly when very large pore size (tens of microns) and extremely high porosity (~80%) are targeted

* Corresponding author at: Department of Chemical and Materials Engineering, Tamsui, Taipei New Taipei city, Hsien 25137, Taiwan. Tel.: +886 2 26215656 x2725/2614; fax: +886 2 26209887.
E-mail address: lpcheng@mail.tku.edu.tw (L.-P. Cheng).

0376-7388/$ - see front matter © 2012 Elsevier B.V. All rights reserved.
http://dx.doi.org/10.1016/j.memsci.2012.05.070

[28,29,31]. For example, Kim and Lee prepared symmetric polycarbonate membranes by template-leaching of polyethylene glycol in supercritical CO_2 fluid. Porosity as high as 72% was achieved; however, the pores were closed in most cases [28]. Using dimethyl sulfone and glycerol as mixed diluents, Wu et al. were able to prepared symmetric polyacrylonitrile membranes by the TIPS method [29]. Both cellular and needle-like pores were obtained with size falling over the range ~2–20 μm, depending on the quenching conditions. However, pore–pore connection was limited to the contact area only, pores were distinctive, and there is no indication of porous channel formation.

In this research, an attempt was made to prepare such special kind of membranes by the NIPS process. The casting solution consisted of Elvamide (a ternary copolymer of Nylon-6, -66, and -610), formic acid, and high molecular weight chitosan, whereas pure water was used as the coagulant. Elvamide is largely amorphous and is much more flexible than its constituent homopolymers [30]. Formation of porous Elvamide membranes by NIPS has been investigated previously [31]. Chitosan, serving as the pore former in the present research, is a biodegradable and biocompatible polysaccharide widely applied in bio-industry [32]. It dissolves in common protic solvents due to protonation of the amine groups on the 2nd carbon of the saccharide ring. Formic acid is a very good solvent for chitosan, as is evident that only 1 wt% formic acid aqueous solution can dissolve the polymer (MW-490,000) at room temperature. This experimental fact renders chitosan a unique pore former for preparing macroporous Elvamide membranes by precipitation from water/formic acid (non-solvent/solvent) solutions. Because chitosan will enter the coagulation bath along with the out-diffusion formic acid during the immersion process, no post-extraction is required to obtain pure Elvamide membranes. Furthermore, it is interesting to find that skinless membranes can be formed thanks to the migration of chitosan, as opposed to common understanding that immersion-precipitation of polyamide in a strong non-solvent, such as water, generally gives rise to asymmetric skinned membranes [6,26,33].

By controlling the ratio of chitosan/Elvamide in the dope, membranes with different porous structures and porosity were obtained. The formed membranes were characterized by ^{1}H NMR, SEM, and tensile strength measurements. Polyamides have been reported to possess good biocompatibility with various human cells and tissues [34–39]. In this research, L929 cells were cultured on the membranes to see their applicability in biotechnology.

2. Materials and methods

2.1. Materials

Elvamide 8601 (copolymer of nylon-6, -66, -610, intrinsic viscosity = 1.761 dl/g, M_v = 56,000, ρ_p = 1.08 g/cm^3) was purchased from Du Pont Engineering Polymers [30]. Chitosan (M_v = 490000, degree of deacetylation = 84%) was purchased from TCI Chemicals. Formic acid (Sigma-Aldrich, 98–100%) was used as the solvent for both Elvamide and chitosan. Distilled and deionized water was used as the non-solvent for precipitation of Elvamide in the immersion process. MTS (3-[4,5dimethylthiazol-2-yl]-5-(3-carboxymethoxyphenyl)-2-(4-sulfophenyl)-2H-tetrazolium), reagent for cell analysis, was purchased from Promega. Formic acid-d_2 (Sigma-Aldrich, 98 at% D) was used as the D-solvent for NMR analysis. All materials were used as received.

Table 1
Conditions for preparation of Elvamide membranes.

Membrane code	Weight of materials in the casting dope (g)			Chitosan/Elvamide ratio	Thickness (μm)
	Elvamide	Chitosan	Formic acid		
M11	11	1.7	98.3	0.155	156.1 ± 7.0
M13	13	1.7	98.3	0.131	156.0 ± 3.1
M15	15	1.7	98.3	0.113	179.8 ± 7.1
M17	17	1.7	98.3	0.100	161.4 ± 7.4

2.2. Elvamide membrane preparation and characterization

A desired amount of pre-dried (in a vacuum oven at 80 °C for 4h) chitosan was dissolved in formic acid at 40 °C on a roller to form a 1.7 wt% polymer solution. To this solution a specific amount (11, 13, 15, or 17 phr) of Elvamide terpolymer was added. The mixture was blended at 45 °C until a clear homogeneous solution was obtained, which took about 12 h. The formed solution was uniformly spread on a glass plate using a casting knife with a clearance of 350 μm. Following casting, the solution was immersed in a water bath

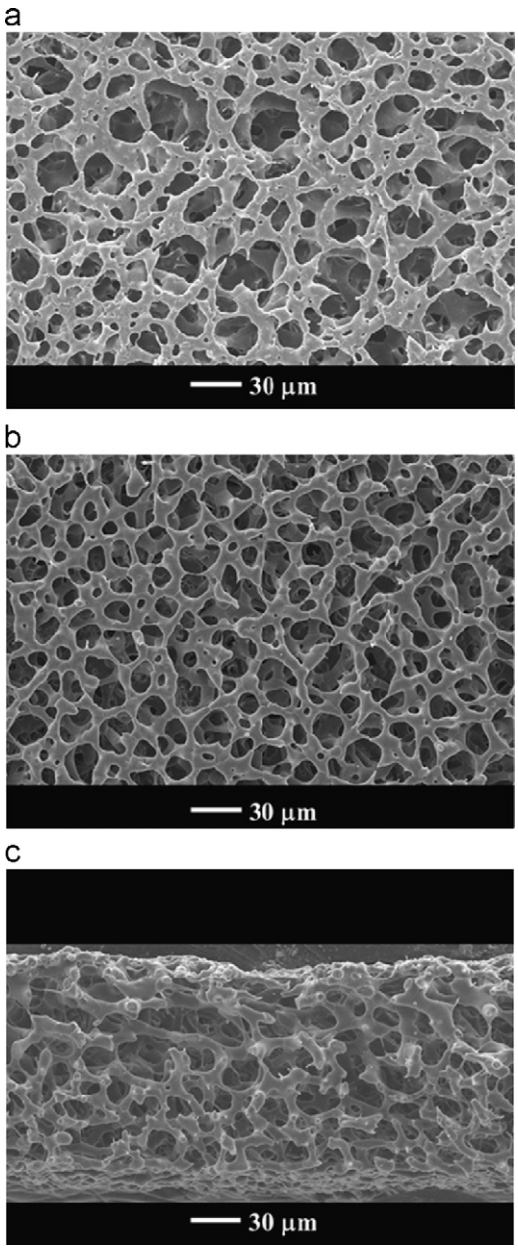

Fig. 1. SEM micrographs of the membrane M11. (a) Top surface; (b) bottom surface; (c) cross-section.

Table 2
Properties of the prepared Elvamide membranes.

Membrane code[a]	Porosity (%)[b]	Mean pore diameter (μm)		Ultimate tensile strength (MPa)	Elongation at break (%)
		Top	Bottom		
M11	82.0 ± 0.5	35.6 ± 6.1	29.7 ± 1.5	1.06 ± 0.10	12.5 ± 2.3
M13	79.6 ± 0.4	29.2 ± 6. 4	19.9 ± 3.3	1.33 ± 0.14	14.2 ± 2.8
M15	78.6 ± 0.3	25.0 ± 4.4	15.9 ± 1.7	2.21 ± 0.15	16.0 ± 1.3
M17	74.4 ± 1.2	17.7 ± 1.8	9.5 ± 1.7	3.25 ± 0.24	16.2 ± 1.8

[a] Membranes formed by wet-phase inversion in deionized water at 10 °C.
[b] Calculated based on the density of Elvamide (1.08 g/cm^3) and the measured mass and thickness of the membrane.

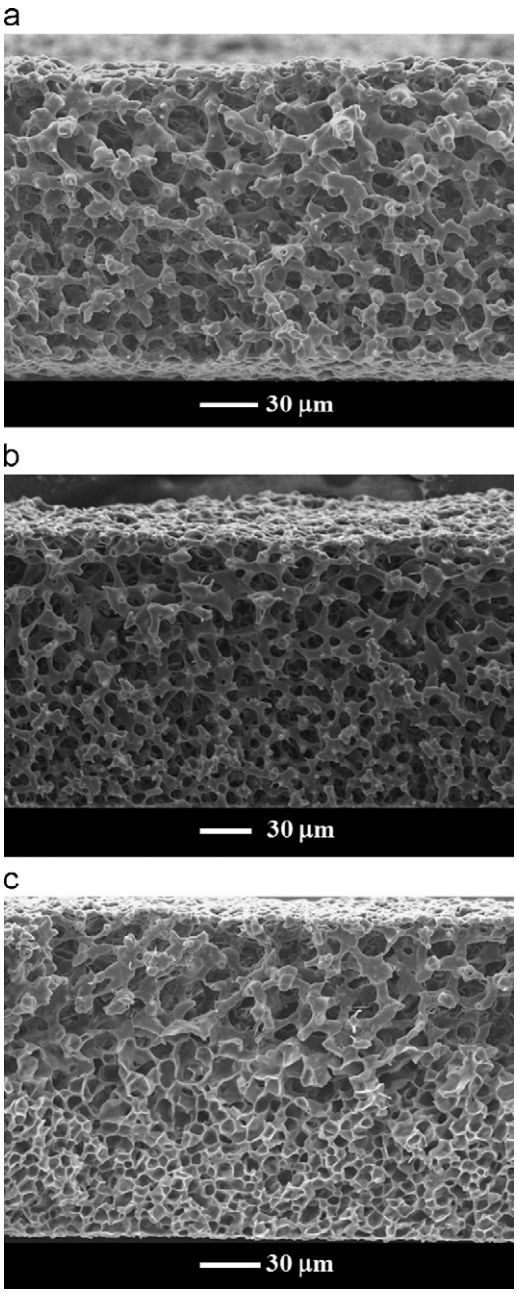

Fig. 2. Cross-sectional morphology of the membranes. (a) M13; (b) M15; (c) M17.

maintained at 10 °C. Typically, precipitation was observed upon immersion as the membrane became turbid or opaque. It was our experience that the development of turbidity required 5–15 s, depending upon the preparation conditions. After the precipitation

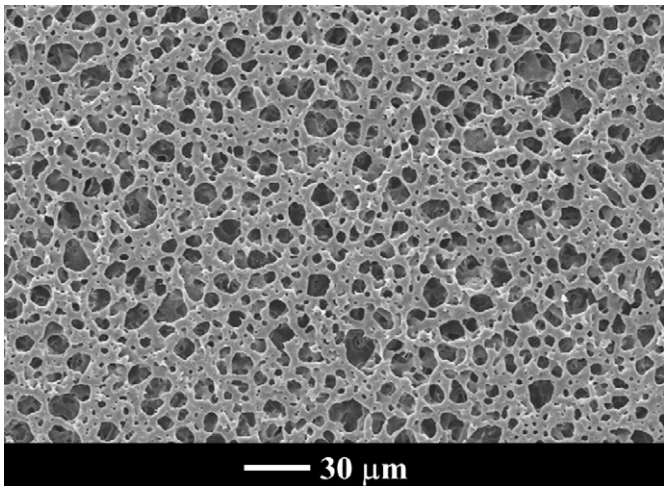

Fig. 3. Morphology of the top surface of the membrane M17.

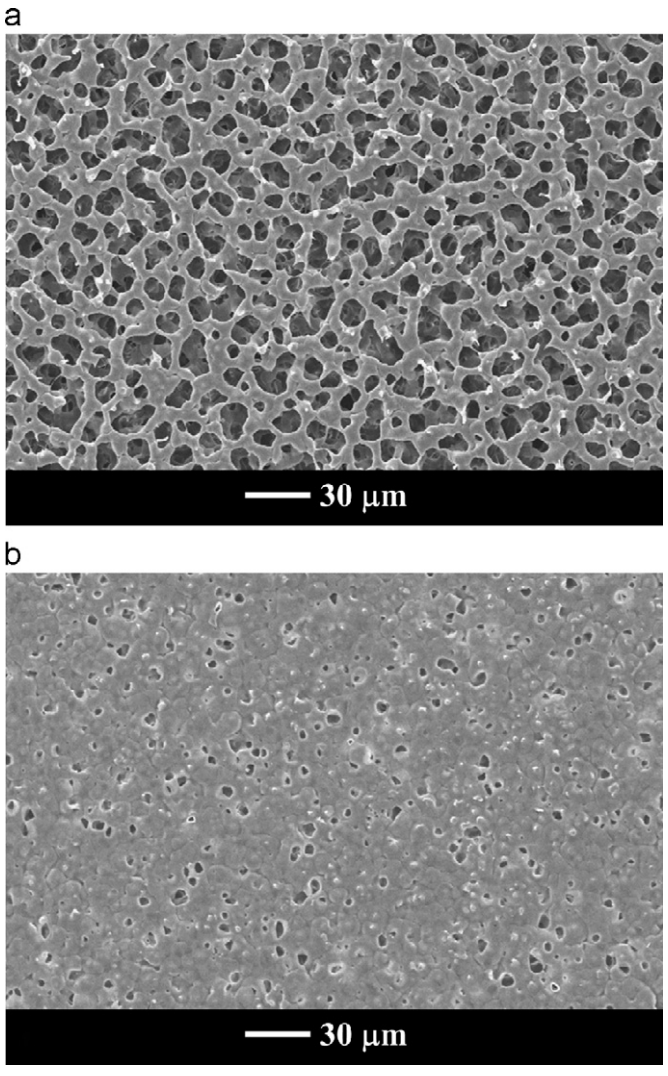

Fig. 4. Morphologies of the bottom surface of the membranes. (a) M13 and (b) M17.

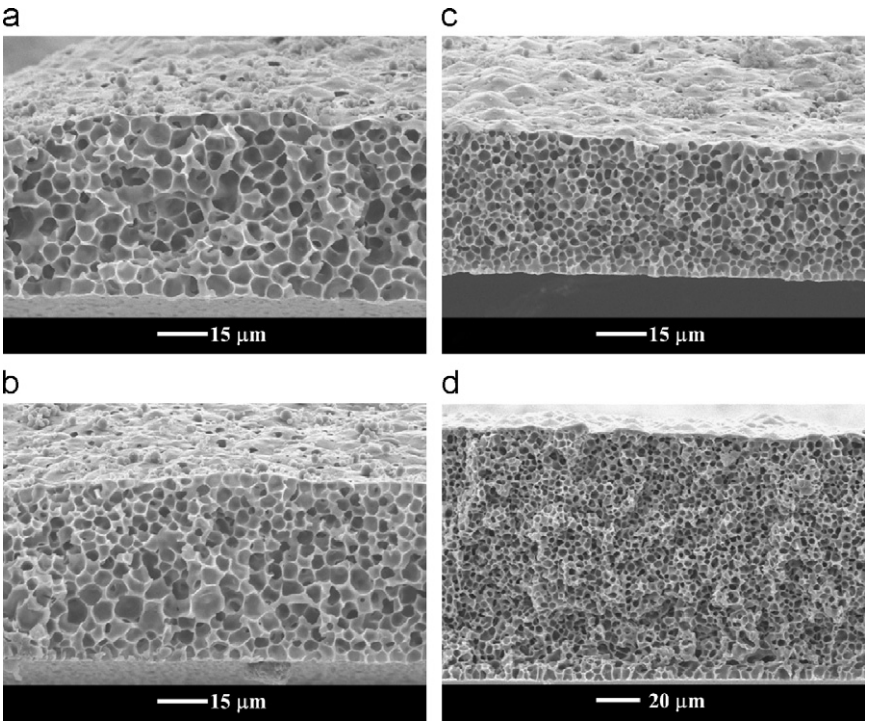

Fig. 5. Cross-sectional morphology of Elvamide membranes prepared without addition of chitosan. Dope polymer composition: (a) 11%; (b) 13%; (c) 15%; (d) 17%.

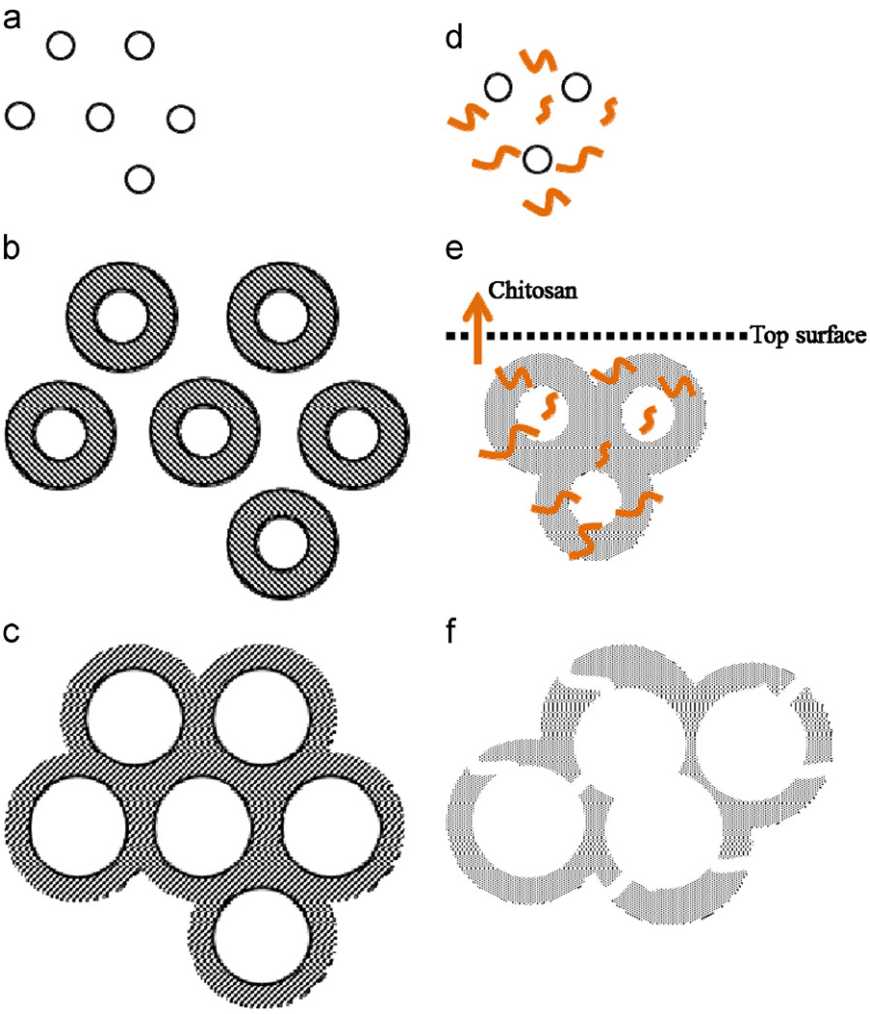

Fig. 6. Schematic representation of the stages of the liquid–liquid phase-separation process. (a) Nucleation; (b) micelle formation; (c) cellular pore formation; (d) liquid nuclei and chitosan chain; (e) micelle and chitosan chain; (f) scaffold-liked structure.

was completed (about 30 min), the nascent membrane was taken out of the bath and washed in distilled water for at least 24 h to remove residual formic acid in the membrane. Finally, the membrane was freeze-dried to avoid collapse of pores in the membrane. The preparation conditions for various membranes are summarized in Table 1. A few methods were employed to characterize the formed membranes.

(1) The porosity of the membrane was determined by the following equation [24]:

$$\text{Porosity}\ (\%) = \left[\frac{V_m - V_e}{V_m}\right] \times 100\% \quad (1)$$

where V_m is the bulk volume of the membrane and V_e is the volume of the polymer. V_m was obtained by multiplying the membrane area by its thickness (measured by a thickness gage). V_e can be calculated by W_m/ρ_p, where W_m is the weight of the membrane and ρ_p is the density of the polymer.

(2) Morphologies of the membranes were observed in top, bottom, and cross-sectional views using a scanning electron microscope (SEM, S-2600H, HITACHI, Japan). The membrane was vacuum-dried and then attached to a sample holder using conductive copper tapes. The cross section of the membrane was obtained by fracturing the membrane in liquid nitrogen. Silver paste was applied at the edges of the sample to enhance electronic conductivity. Then, the sample was sputtered with a thin layer of gold and observed under an acceleration voltage of 10 kV.

(3) ^{1}H NMR spectroscopy was used to see whether all chitosan had left the membrane during the immersion-precipitation

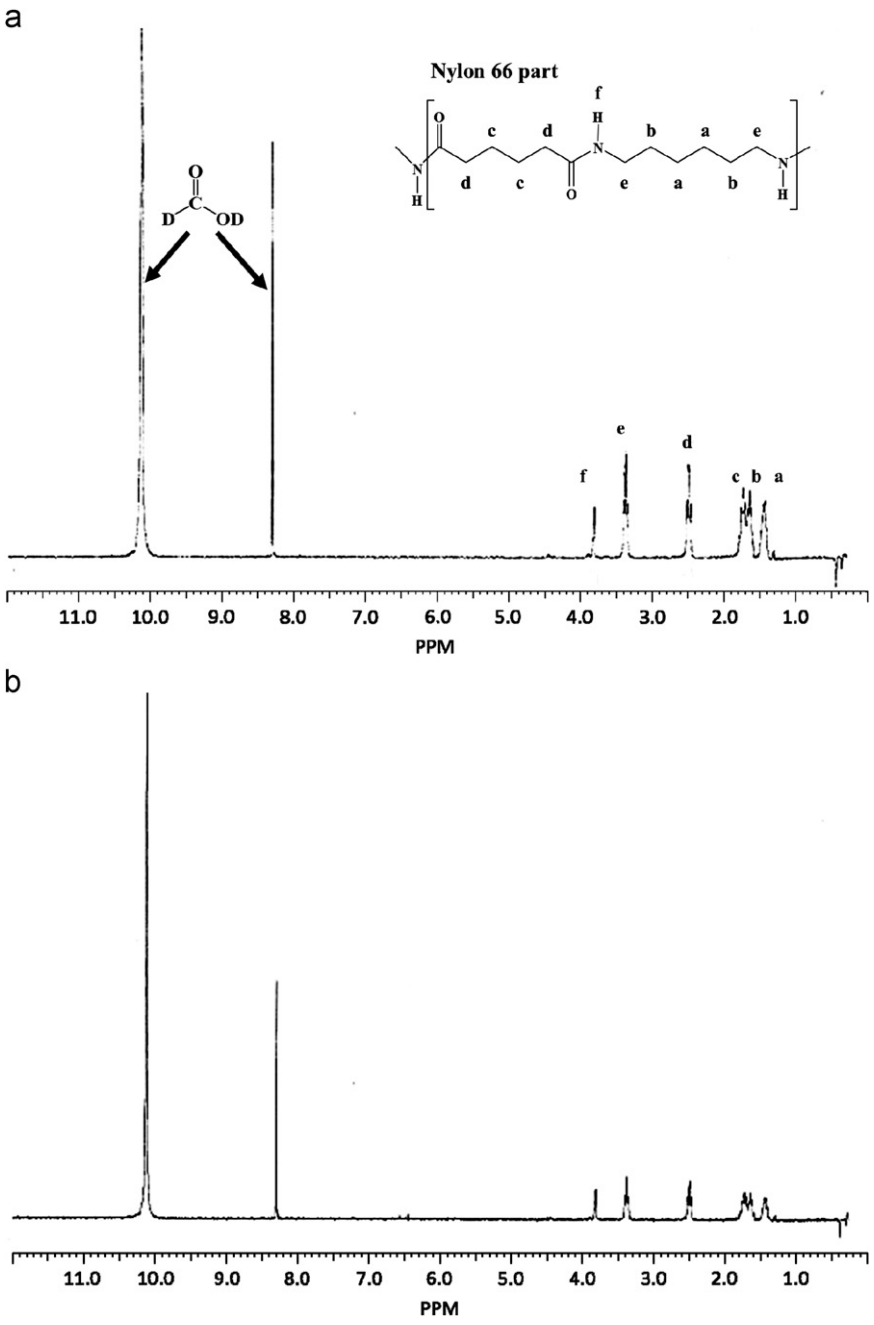

Fig. 7. ^{1}H NMR spectra of (a) Pure Elvamide and (b) M17.

process. The spectra were obtained on a Bruker AC-300 FT-NMR instrument (Germany) operated at 300 MHz. D_2-formic acid was used as the solvent for both polymers.

(4) Pore size of the membranes was determined using image analysis software (Image J, National Institutes of Health, USA) on SEM micrographs. The ranges of pore area and circularity were set to 20–infinity μm^2 and 0.6–1.0, respectively. For each membrane, analyses were made on 5 different SEM micrographs and the average value was reported together with deviations.

(5) Tensile strength and elongation at break (Shimadzu, AGS-J, Japan) for various membranes were measured following ASTM D638–91.

2.3. Cell culture

Mouse fibroblast-like cells (L929) were suspended in DMEM (Gibco/Invitrogen, California, USA) and cultured in a humidified atmosphere of 95% air and 5% CO_2 at 37 °C. The medium was renewed every 2 days. The membranes were secured in the wells of tissue-culture treated polystyrene plates (TCPS). Subsequently, cell suspension with a cell concentration of about 1×10^5/ml was added to each well. After incubation for various periods, cells attached on the membranes were harvested for analysis. 20 μL MTS was pipetted into each well and incubated for 4 h at 37 °C. The number of cells was determined based on the values of OD_{490} with a micro-plate spectrophotometer (ELISA, Multickan Spectrum, Thermo Science, UK). Furthermore, cells stained by DAPI (diamidino-2-phenylindole) were observed using a fluorescence microscope to see the distribution of cells on the membrane [40].

3. Results and discussion

3.1. Morphologies of the membranes

Fig. 1 shows the SEM images of the membrane M11. The membrane exhibits the so-called lacy-like bi-continuous morphology, composed of two interwoven networks with one being macroporous channels of pore size ~30–40 μm, and the other being polymer matrix. As far as our knowledge is concerned, bi-continuous morphology of such pore-size scale and pore–pore connectivity has never been reported in the membrane literature. The top and bottom surfaces are porous with a slight difference in pore size (cf. Table 2), which is related to the escaping activity of chitosan during the immersion-precipitation process, as will be discussed later. Experimentally, it is noted that the top surface is not smooth; deep troughs (some tens of μm) are frequently observed. For example, a vertical depression of 20 μm over the length of 130 μm can be seen in Fig. 1(c). Although a bi-continuous Elvamide membrane has been demonstrated previously [31,41], it should be noted that the membrane had smaller pore size and was prepared by the very slow "vapor-induced phase separation" process suggested by Paine [41]. For the present immersion precipitation process (in water bath), it is impossible to form bi-continuous structure without participation of chitosan.

The Elvamide content in the casting dope has a significant effect on the morphology of the formed membrane, as illustrated in Figs. 2–4. Fig. 2 depicts the cross sectional images of the membranes prepared by dopes containing 13, 15, and 17 phr of Elvamide. The membranes M13 and M15 still hold the bi-continuous feature, while the membrane M17 loses the pore–pore continuity on the bottom half of the cross section. The pore size is found to decrease with increasing Elvamide content in the dope. Specifically, the pore size near the top surface of the membrane M11 is about 30 μm; yet, it becomes 15 μm for M17. Despite such significant difference in pore size, all membranes have a similar porosity, around 80%, suggesting that the number of pores in the membrane increases from the membrane M11 to M17. It is also interesting to find that the top surface of the membranes M13–M17, as opposed to M11, is smooth and free of visible indentation or pin-holes. That is, higher Elvamide fraction helps to hold the mechanical integrity of the membrane against possible surface rupture caused by escaping chitosan molecules. When the Elvamide content in the dope reaches 17 phr, as shown in Fig. 2(c), the lower-half of the membrane evolves into the closed-cell morphology typical of amorphous membranes prepared by the non-solvent induced phase separation process [31]. Because the cellular pores are not inter-connected, the membrane is impenetrable with respect to micron-sized objects.

Just as the membrane M11, the top surface of the other membranes is also porous, however, with a smaller pore size. As an example, Fig. 3 shows the top surface view of the membrane M17. The pores are more or less circular, evidencing the occurrence of liquid–liquid demixing event just underneath the membrane-bath interfacial layer. The pore size distributes over the range 10–40 μm, with an average of 18 μm, only about 1/2 of those on the top surface of the membrane M11. This is consistent with the general observation that more concentrated dope gives rise to smaller pore size [42–45]. Elvamide content affects the pore size of the bottom surface with a trend similar to the top surface. The bottom surface images of the membranes M13 and M17 in Fig. 4 illustrate this point. The pore size of the membrane M13 is on average 20 μm, and there is good connectivity between the pores. In contrast, the bottom surface of membrane M17 is not very porous, containing more dense regions than porous ones. If not with

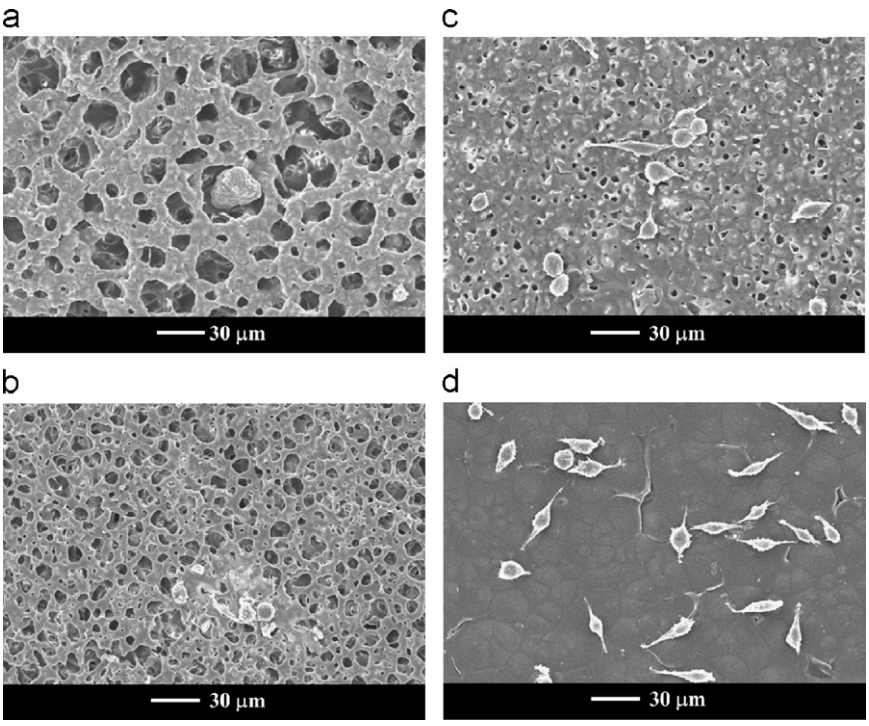

Fig. 8. SEM micrographs of L929 cells cultured on Elvamide membrane surfaces. (a) M13T; (b) M17T; (c) M17B; (d) MD.

the small fraction of isolated pores, this surface may be termed a dense skin. In summary, the Elvamide/chitosan ratio appears to play an important role on the morphology of the immersion-precipitated membranes. It is crucial to have the Elvamide content less than 15 phr, in case that highly bi-continuous porous membrane is sought to produce.

3.2. Bi-continuous structure formation

A preliminary formation process for the bi-continuous structure is proposed herein. To understand why incorporation of chitosan in the dope promotes pore–pore inter-connection, it is instructive to examine the morphologies of pure Elvamide membranes prepared without involving chitosan. Such cases are demonstrated in Fig. 5. The casting dopes comprised 11%, 13%, 15%, or 17% Elvamide in formic acid, and the bath was pure water. It can be seen that all the membranes possess a cellular cross-section, typical of amorphous membranes formed from nonsolvent induced phase separation [31]. The size of the cellular pore decreases with increasing Elvamide concentration. The formation mechanism of the cellular morphology has been described previously [31]. Here, it is briefly introduced, as it is related to the formation of chitosan-induced bi-continuity in the membranes. The precipitation process (free of chitosan) is shown schematically in Fig. 6. The liquid–liquid demixing process begins with the nucleation of liquid domains, Fig. 6(a). These domains (composed of water and formic acid) are enclosed in a polymer-rich concentration boundary layer, Fig. 6(b). The encapsulated domains grow as a result of diffusional influx of the solvent and non-solvent from the bulk solution. Radial growth of the domains occurs and is accompanied by thickening of the amorphous polymer-rich boundary layer. This process continues until a gelation stage is reached, at which the polymer chains in the boundary layers touch, entangle, and then fuse into a continuous polymer gel matrix, in which micro-drops are dispersed Fig. 6(c). [31].

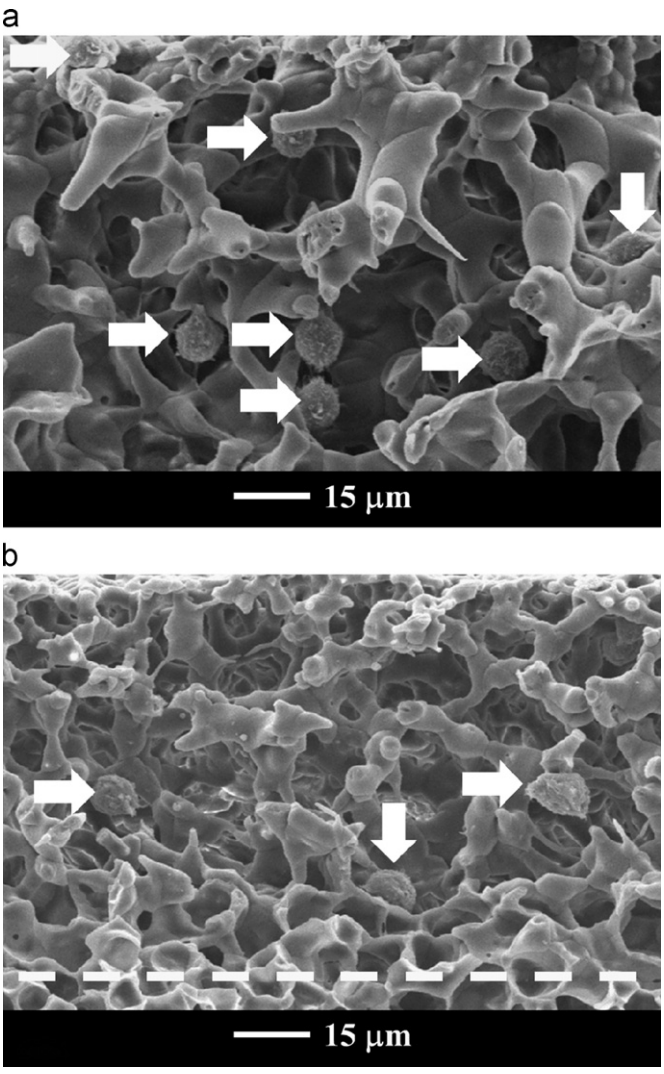

Fig. 9. SEM micrographs of L929 cells cultured on Elvamide membranes cross sectional view. (a) M13T and (b) M17T.

Chitosan is known to interact strongly with water and formic acid through hydrogen bondings; as is evident, chitosan/formic acid casting dope dissolves in water bath (i.e., the casting dope disappears) soon after immersion. In other words, during the immersion-precipitation process, chitosan tends strongly to leave the casting solution along with the out-diffusing formic acid (the NMR analysis proves this point). This activity interferes with the nucleation and growth of domains. At the very start of nucleation, most chitosan chains may still be expanded and spread uniformly in the dope solution, Fig. 6(d), where out-flux of formic acid is limited to the top surface. As the domains grow, some chitosan chains will enter the domains (composed of formic acid and water) just as they migrate into the bath, which causes the polymer-rich boundary layer to break open, Fig. 6(e). Eventually, chitosan molecules will all be leached-out, leaving numerous connective channels between pores to yield a scaffold-like structure, Fig. 6(f). However, it is noted that when the chitosan content is lower than a critical value (e.g., M17), all chitosan will leave the membrane before full development of cellular pores; especially, towards the bottom surface of the membrane. Thus, in this region, only ordinary cellular structure is formed, and the membrane appears like the asymmetric Elvamide membrane shown in Fig. 5(d). Fig. 2 also indicates that the pore size of the membrane decreases gradually along the cross-section. This further evidences the out-diffusion behavior of chitosan during membrane formation.

3.3. Chitosan leaching analysis

Fig. 7 shows the ^{1}H NMR spectra of the pure Elvamide polymer and the formed porous membrane M17. The two sharp peaks at 8.3 ppm and 10.2 ppm are due to the resonance of deuterium of formic acid-d_2. With reference to the spectrum of Nylon 66, the peaks in Fig. 7 can be assigned [46]. The NH proton resonates at the chemical shift $\delta \approx 3.8$ ppm. The five kinds of methylene protons (a–e) correspond to the peaks at 1.2, 1.6, 1.7, 2.5, and 3.3 ppm. Comparing Fig. 7(a) and (b), it can be seen that the chemical shifts of these two spectra are exactly the same. Moreover, from the ^{1}H NMR data of chitosan [47–52], the characteristic peaks, e.g., 2.1 ppm for CH_3 of NHAc, and 4.80 ppm for H-1 of GlcN residue, are not observed in Fig. 7(b). Thus, it may be inferred that chitosan has been leached out completely during the immersion-precipitation process.

3.4. Porosity and tensile strength of the membranes

The porosities of the formed membranes are listed in Table 2. For all membranes, the porosities are exceptionally high, over the range of 74–82%, compared with ~60% for common microfiltration membranes. The porosity of the membrane M17 is somewhat smaller than the other three membranes primarily due to the presence of closed-cellular structure on the bottom half of the membrane. To prepare highly porous membranes, the mechanical strength is a major issue to account for. It is interesting to find that all the prepared membranes have tensile strengths high enough for cell culture applications, as shown in Table 2. This can be attributed to the inter-connectivity associated with the bi-continuous structure. The tensile strength of the membrane M11 is 1.06 MPa, the lowest of the four membranes, due to its high porosity and large pore size. For the membrane M17, tensile strength as high as 3.25 MPa is achieved, which can be attributed to the lower porosity and presence of a cellular region on the bottom half of the membrane. As regarding the elongation at break, the same tendency as the tensile strength is found; however, it increases with a smaller scale from M11

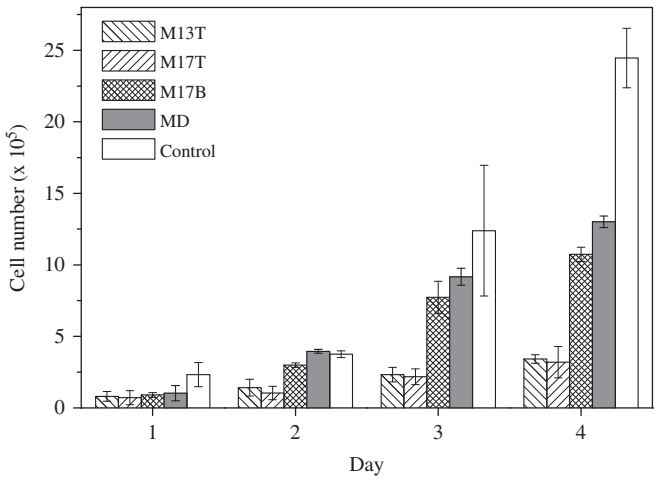

Fig. 10. Cell number of L929 cells cultured on different Elvamide membrane surfaces by MTS assay.

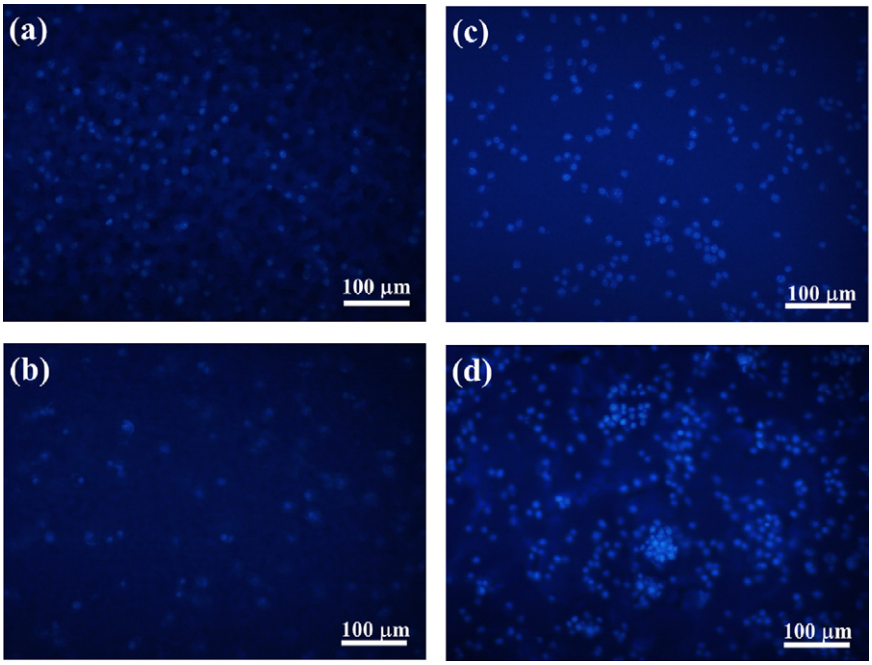

Fig. 11. L929 cells cultured on different Elvamide membrane surfaces, stained with DAPI. (a) M13T; (b) M17T; (c) M17B; (d) MD.

to M17. The porosity, pore size, and cellular structure are considered to be responsible for this result.

3.5. Cell culture for prepared membranes

L929 cells were cultured on various membrane surfaces to see the effect of pore size and morphology on the response of the cells. The employed surfaces include the top surfaces of the membranes M13 and M17 (termed M13T and M17T, respectively), the bottom surface of the membrane M17 (termed M17B), and the surface of a dense Elvamide film (termed MD). They are chosen so as to cover a wide range of pore size. Fig. 8 shows the SEM images of the cells cultured on these surfaces for 4 days. It appears that L929 cells attach and proliferate well on M17B and MD. Most of the cells on MD have grown into the shape of a spindle, while on M17B globular cells are still observable. Out-stretching of pseudopodia is observed on both membranes. However, quite different situation is encountered for the cases of culturing on M13T and M17T. As indicated in Fig. 8 (a) and (b), instead of growing on top of the surface, the cells tend to enter the porous channels in the cross-sectional region. The close-up views in Fig. 9(a) and (b) demonstrate clearly the adherence of the cells to the pore wall. Such clear in-growth behavior has never been demonstrated in the literature. These cells are of spherical shape and there is no evidence of pseudopodia extension. The size of the cells, ~10 μm, is somewhat smaller than those on M17B or MD. Thus, a negative effect is implied for L929 to grow in a channel-like confined environment. Also, because the cellular pores beneath the bi-continuous part of M17 are all closed, no cell is detected in this region.

Fig. 10 depicts the cell number determined by MTS analysis over the culturing period of 4 days. For the porous surfaces M13T and M17T, the population of cell increases slowly, and at the end it is only about three times the initial seeded level. In contrast, those cultured on denser surfaces M17B and MD undergo significant number changes along the course; e.g., on the 2nd day, the cell numbers are already slightly larger than the final cell number on M13T and M17T. This suggests that a dense surface is more favorable for the growth of L929 cells than a porous surface, which is consistent with previous results that osteoblastic cell prefers to adhere to a rough/porous surface, whereas the fibroblast prefers a smooth one. Although dense surface may be more suited to L929, the fact that cells can reside and grow in the porous channels deserves some attention.

Fig. 11 depicts the DAPI-stained optical images of cells on various membranes after 4 days in culture. The population of the cell agrees with the MTS data, namely, MD > M17B > M13T ~ M17T. Furthermore, cells are largely separated for culturing on M13T and M17T; yet, considerable aggregation of the cells occurs on MD and M17B. For the former case, the cells may have entered the pores initially and may reside at different sites in the 3-D skeleton. They grow independently, facing geometric obstructions, to give the shape of a sphere. On the other hand, on the denser membranes, the cells attach firmly and undergo 2-D growth with considerable pseudopodia extension and cell proliferation.

4. Conclusion

Preparation of Elvamide membranes by the wet-phase inversion method, using chitosan as a pore former, was investigated. The formed membranes exhibit bi-continuous morphologies with high porosities and large pore sizes that are rarely reported in the membrane literature. By manipulating the chitosan/Elvamide ratio in the dope, membranes with different morphologies can be obtained. When this ratio is increased, the pore size and the porosity of the formed membrane decrease, while the tensile strength increases. In the extreme case, porosity as high as 82% can be established at the chitosan/Elavamide ratio of 15.5%. As a pore former, chitosan is completely removed from the membrane during the precipitation process, as is validated by the ^{1}H NMR analysis. The biological compatibility of the prepared membranes has also been examined via culturing of the L929 cells. The cells are able to attach and grow in the porous channels in the membrane cross section, however, with a lower proliferation than those cultured on a smooth surface.

Acknowledgments

The authors thank the National Science of Council for financial support (NSC 99–2221-E-032–002-MY1).

Reference

[1] M. Nakashima, A. Akamine., The application of tissue engineering to regeneration of pulp and dentin in endodontics, J. Endod 31 (2005) 711–718.
[2] G.P. Chen, Y. Ushida, T. Tateishi, Scaffold design for tissue engineering, Macromolecular Biosci. 2 (2002) 67–77.
[3] M.H. Ho, P.Y. Kuoa, H.J. Hsieha, T.Y. Hsien, L.T. Hou, J.Y. Lai, D.M. Wang, Preparation of porous scaffolds by using freeze-extraction and freeze-gelation methods, Biomaterials 25 (2004) 129–138.
[4] H. Lee, W.B. Krantz, S.T. Hwang., A model for wet-casting polymeric membranes incorporating nonequilibrium interfacial dynamics, vitrification and convection, J. Membr. Sci. 354 (2010) 74–85.
[5] D.J. Lin, L.P. Cheng, S.P. Lin, Effect of compatible nucleation seeds on the morphology of porous Nylon 6 membrane, Desalination 145 (2002) 31–37.
[6] T.H. Young, D.J. Lin, J.J. Gau, W.Y. Chuang, L.P. Cheng, Morphology of crystalline Nylon-610 membranes prepared by the immersion-precipitation

process: competition between crystallization and liquid–liquid phase separation, Polymer 40 (1999) 5011–5021.
[7] A. Dufresne, J. Cavaillé, D. Dupeyre, M. Garcia-Ramirez, J. Romero, Morphology, phase continuity and mechanical behaviour of polyamide 6/chitosan blends, Polymer 40 (1999) 1657–1666.
[8] Č. Stropnik, V. Musil, M. Brumen, Polymeric membrane formation by wet-phase separation; turbidity and shrinkage phenomena as evidence for the elementary processes, Polymer 41 (2000) 9227–9237.
[9] Č. Stropnik, V. Kaiser, Polymeric membranes preparation by wet phase separation: mechanisms and elementary processes, Desalination 145 (2002) 1–10.
[10] D.J. Mooney, D.F. Baldwin, N.P. Suh, L.P. Vacanti, R. Langer, Novel approach to fabricate porous sponges of poly (d,L-lactic-coglycolic acid) without the use of organic solvents, Biomaterials 17 (1996) 1417–1422.
[11] L.D. Harris, D.F. Baldwin, D.J. Mooney, Open pore biodegradable matrices formed with gas foaming, J. Biomed. Mater. Res. 42 (1998) 396–402.
[12] A.R.R. Jose, M.T. Jean, P. Matthieu, D. Michel, Two-step micro cellular foaming of amorphous polymers in supercritical CO_2, J. Supercritical Fluids 57 (2011) 87–94.
[13] Y.J. Park, K.H. Nam, S.J. Ha, Porous poly (L-latide) membranes for guided tissue regenerarion and controlled drug delivery: membrane fabrication and characterization, J. Control Release 43 (1997) 151–160.
[14] Y.H. Zhao, B.K. Zhu, X.T. Ma, Y.Y. Xu, Porous membranes modified by hyperbranched polymers. I: Preparation and characterization of PVDF membrane using hyperbranched polyglycerol as additive, J. Membr. Sci. 290 (2007) 222–229.
[15] L.Z. Zhang, Coupled heat and mass transfer through asymmetric porous membranes with finger-like macrovoids structure, Int. J. Heat Mass Transfer 52 (2009) 751–759.
[16] D.J. Lin, C.L. Chang, F.M. Huang, L.P. Cheng, Effect of salt additive on the formation of microporous poly(vinylidene fluoride) membranes by phase inversion from LiClO4/Water/DMF/PVDF system, Polymer 44 (2003) 413–422.
[17] J.S. Park, S.K. Kim, K.H. Lee, Effect of $ZnCl_2$ on formation of asymmetric PEI. Membrane by phase inversion process, J. Ind. Eng. Chem. 6 (2000) 93–99.
[18] G. Chen, T. Ushida, T. Tateishi., A biodegradable hybrid sponge nested with collagen microsponges, J. Biomed. Mater. Res. 51 (2000) 273–279.
[19] J. Ma, H. Wang, B. He, J. Chen., A preliminary in vitro study on the fabrication and tissue engineering applications of a novel chitosan bilayer material as a scaffold of human neofetal dermal fibroblasts, Biomaterials 22 (2001) 331–336.
[20] A. Rahimpour, S.S. Madaeni, Y. Mansourpanah, Fabrication of polyethersulfone (PES) membranes with nano-porous surface using potassium perchlorate ($KClO_4$) as an additive in the casting solution, Desalination 258 (2010) 79–86.
[21] D.E.S. Santos, C.G.T. Neto, J.L.C. Fonseca, M.R. Pereira, Chitosan macroporous asymmetric membranes—Preparation, characterization and transport of drugs, J. Membr. Sci. 325 (2008) 362–370.
[22] K. Whang, C.H. Thomas, K.E. Healy, G. Nuber, A novel method to fabricate bioabsorbable scaffolds, Polymer 36 (1995) 837–842.
[23] G. Chen, T. Ushida, T. Tateishi, Preparation of poly(L-lactic acid) and poly(DL-lactic-co-glycolic acid) foams by use of ice microparticulates, Biomaterials 22 (2001) 2563–2567.
[24] H.H. Chang, L.C. Yao, D.J. Lin, L.P. Cheng, Preparation of microporous poly(VDF-co-HFP) membranes by template-leaching method, Sep. Purif. Technol. 72 (2010) 156–166.
[25] J.P. Zheng, C.Z. Wang, X.X. Wang, H.Y. Wang, H. Zhuang, K.D. Yao, Preparation of biomimetic three-dimensional gelatin/montmorillonite–chitosan scaffold for tissue engineering, React. Funct. Polym. 67 (2007) 780–788.
[26] C. Stropnik, A. Car, Some aspects of polymeric asymmetric porous membranes formation by wet-phase separation method, Desalination 199 (2006) 130–132.
[27] J. Yang, G. Shi, J. Bei, S. Wang, Y. Cao, Q. Shang, G. Yang, W. Wang, Fabrication and surface modification of macroporous poly(L-lactic acid) and poly(L-lactic-co-glycolic acid) (70/30) cell scaffolds for human skin fibroblast cell culture, J. Biomed. Mater. Res. 62 (2002) 438–446.
[28] M.S. Kim, S.J. Lee, Characteristics of porous polycarbonate membrane with polyethylene glycol in supercritical CO_2 and effect of its porosity on tearing stress, J. Supercritical Fluids 31 (2004) 217–225.
[29] Q.Y. Wu, L.S. Wan, Z.K. Xu, Structure and performance of polyacrylonitrile membranes prepared via thermally induced phase separation, J. Membr. Sci. 409–410 (2012) 355–364.
[30] DuPont™. ElvamideR resins: Products and Properties Guide.
[31] C.H. Shih, C.C. Gryte, L.P. Cheng, Morphology of membranes formed by the isothermal precipitation of polyamide solutions from water/formic acid systems, J. Appl. Polym. Sci. 96 (2005) 944–960.
[32] M.N.V. Ravi Kumar, A review of chitin and chitosan applications, React. Funct. Polym. 46 (2000) 1–27.
[33] D.J. Lin, C.C. Chang, C.K. Lee, L.P. Cheng, Fine structure and crystallinity of porous Nylon 66 membranes prepared by phase inversion in the water/formic acid/Nylon 66 system, Eur. Polymer J. 42 (2006) 356–367.
[34] R. Nirmala, R. Navamathavan, H.S. Kang, M.H. El-Newehy, H.Y. Kim, Preparation of polyamide-6/chitosan composite nanofibers by a single solvent system via electrospinning for biomedical applications, Colloids Surf., B 83 (2011) 173–178.
[35] S.J. Lin, W.C. Hsiao, S.H. Jee, H.S. Yu, T.F. Tsai, J.Y. Lai, T.H. Young, Study on the effects of nylon–chitosan-blended membranes on the spheroid-forming activity of human melanocytes, Biomaterials 27 (2006) 5079–5088.
[36] R. Nirmala, H.M. Park, R. Navamathavan, H.S. Kang, M.H. El-Newehy, H.Y. Kim, Lecithin blended polyamide-6 high aspect ratio nanofiber scaffolds via electrospinning for human osteoblast cell culture, Mat. Sci. Eng.: C 31 (2011) 486–493.
[37] H. Wang, Y. Li, Y. Zuo, J. Li, S. Ma, L. Cheng, Biocompatibility and osteogenesis of biomimetic nano-hydroxyapatite/polyamide composite scaffolds for bone tissue engineering, Biomaterials 28 (2007) 3338–3348.
[38] W. Jie, L. Yubao., Tissue engineering scaffold material of nano-apatite crystals and polyamide composite, Eur. Pol. J. 40 (2004) 509–515.
[39] S. Das, S.J. Hollister, C. Flanagan, A. Adewunmi, K. Bark, C. Chen, K. Ramaswamy, D. Rose, E. Widjaja, Freeform fabrication of Nylon-6 tissue engineering scaffolds, Rapid Prototyping J. 9 (1) (2003) 43–49.
[40] D.J. Jung, A. Al-Ahmad, M. Follo, B. Spitzmuller, W. Hoth-Hannig, M. Hannig, C. Hannig, Visualization of initial bacterial colonization on dentine and enamel in situ., J. Microbiol. Methods 81 (2010) 166–174.
[41] R.A. Paine. U.S. Pat. 3408315 (1968).
[42] Gh. Bakeri, A.F Ismail, M. Shariaty-Niassar, T. Matsuura, Effect of polymer concentration on the structure and performance of polyetherimide hollow fiber membranes, J. Membr. Sci. 363 (2010) 103–111.
[43] Y. Tang, N. Li, A. Liu, S. Ding, C. Yi, H. Liu, Effect of spinning conditions on the structure and performance of hydrophobic PVDF hollow fiber membranes for membrane distillation, Desalination 287 (2012) 326–339.
[44] E. Yuliwati, A.F. Ismail, Effect of additives concentration on the surface properties and performance of PVDF ultrafiltration membranes for refinery produced wastewater treatment, Desalination 273 (2011) 226–234.
[45] P. van de Witte, p.j. Dijkstra, J.W.A. van den Berg, J. Feijen, Phase separation processes in polymer solutions in relation to membrane formation, J. Membr. Sci. 117 (1996) 1–31.
[46] M.R. Krejsa, K. Udipi, J.C. Middleton., NMR analysis of UV- and heat-aged Nylon-6,6, Macromolecules 30 (1997) 4695–4703.
[47] M.R. Kasaai, Determination of the degree of N-acetylation for chitin and chitosan by various NMR spectroscopy techniques: A review, Carbohydr. Polym. 79 (2010) 801–810.
[48] R.S. Jagadish, K.N. Divyashree, P. Viswanath, P. Srinivas, B. Raj, Preparation of N-vanillyl chitosan and 4-hydroxybenzyl chitosan and their physico-mechanical, optical, barrier, and antimicrobial properties, Carbohydr. Polym. 87 (2012) 110–116.
[49] W. Ding, Q. Lian, R.J. Samuels, M.B. Polk, Synthesis and characterization of a novel derivative of chitosan, Polymer 44 (2003) 547–556.
[50] S. Kumar, J. Koh, H. Kim, M.K. Gupta, P.K. Dutta, A new chitosan–thymine conjugate: Synthesis, characterization and biological activity, Int. J. Biol. Macromol. 50 (2012) 493–502.
[51] B. Yun Yang, R. Montgomery, Degree of acetylation of heteropolysaccharides, Carbohydr. Res. 323 (2000) 156–162.
[52] M. Monier, Y. Wei, A.A. Sarhan, Evaluation of the potential of polymeric carriers based on photo-crosslinkable chitosan in the formulation of lipase from Candida rugosa immobilization, J. Mol. Catal B 63 (2010) 93–101.